Spring 5-1995

Fracture Patterns of Human Cadaver Long Bones

Jennie Patricia Psihogios
University of Tennessee - Knoxville

FRACTURE PATTERNS OF HUMAN CADAVER LONG BONES

Tyler A. Kress[1], David J. Porta[2,3], John N. Snider[1], Peter M. Fuller[3], Jennie P. Psihogios[1], Wendy L. Heck[2], Stephen J. Frick[2], Jack F. Wasserman[1]

[1] University of Tennessee - Knoxville, Tennessee USA
[2] Bellarmine College - Louisville, Kentucky USA
[3] University of Louisville School of Medicine - Louisville, Kentucky USA

ABSTRACT

A primary objective of this experimental investigation was to further understand relationships among loading characteristics as they affect the resultant fractures of human long bones (tibia, femur, humerus, and fibula). Numerous human cadaver long bones were loaded in controlled laboratory conditions with varying test parameters such as loading direction, specimen choice, impact velocity, and test method. Data presented in this paper focus on the resultant fracture patterns for the tibia and femur tests. Observations were made based on these data and on the authors' general knowledge with respect to fracture behavior. These comments draw upon a decade of laboratory experience of dynamically loading human cadaver long bones.

ALL PERSONS ARE AT RISK for fractures, especially to the long bones. This is true for young persons, who generally may otherwise be healthy, and older persons, in which osteoporotic and arthritic changes can increase the seriousness of such fractures. Most fractures heal successfully, but many result in significant loss of function and permanent disability. Some of the complications are directly related to the fracture itself, but others are associated with accompanying effects of the fracture. The fractured bone may pierce the skin creating an open wound possibly resulting in infection, or may lead to other injuries involving the surrounding neurologic, vascular, and connective tissues. The primary sources of such injuries are the jagged edges of the fractured components and displaced bone fragments. Potential post-traumatic impairments may include arthritis, chronic pain, decreased weight-bearing capacity, limited range of motion, and osteodeformities.

An understanding of long bone failure mechanisms and fracture patterns is helpful in characterizing the resultant injuries. Also, more knowledge with respect to failure mechanisms can facilitate development of better "systems" or "environments" to minimize severity of injuries.

Breaking strength and fracture patterns of long bones have been studied quite extensively with good documentation dating as far back as the 19th century. Messerer (1880) tested 500 bones from 90 cadavers of both sexes and various ages. He found that the cracking or tearing of the bone generally occurred on the convex (tension) side of the bone. In bones exhibiting significant bend there was crushing on the concave (compression) side, at the point of application of the load, before a tearing or tension fracture occurred. The significance of tensile stresses as the cause for bone failure was further emphasized by Evans and Lissner (1948) through stresscoat studies. Mechanical property studies over the years have shown that bone is weaker in tension than in compression. Rauber (1876) was one of the first researchers to discover that when a bone is subjected to increasing amounts of equal tensile and compressive forces it fails in tension first. Kress and Porta (1993) have found that the human femur seems to be approximately 1.5 times stronger in compression than tension, even during dynamic loading conditions.

A fracture, or break in the surface of a bone, can range from a simple crack to complete rupture of the bone structure with fragmentation. Injury severity, as it relates to fractures, depends on three primary parameters: fracture location, degree of displacement of the broken bone or associated fragments, and nature of the surrounding soft tissues and skin. These parameters are variable depending on the specific loading situation.

Long bone fractures occur to the diaphysis (shaft) and/or the epiphyses (articular regions). The shaft is usually discussed in terms of three equal subdivisions of the bone's length. The third closest to the torso is described as "proximal", the middle third is simply "the middle third," and the third furthest from the torso is described as "distal."

Open fractures, as opposed to closed, involve damage to the overlying skin and, naturally, the adjacent soft tissue structures. These fractures usually result in increased blood loss, decreased healing rates, and greater risk of infection. This increased risk of infection is supported by Dellinger et al (1988) in a study of 240 patients. Roth et al (1986) reviewed infectious morbidity in 838 patients and found that infection was prevalent 8% more often with open fractures as compared to closed.

Comminuted (i.e. bone is broken into more than two pieces) is another type of fracture that can cause significant soft tissue damage. Varying degrees of comminution manifest as relatively simple wedges or segmental fractures to more complex longitudinal split or massively fragmented fractures (as illustrated in Figure 1). Also shown in Figure 1 are the common non-comminuted fracture patterns: transverse, oblique, and spiral. Other descriptions of fractures (e.g. impacted, avulsion, greenstick, etc.) will not be discussed due to the scope of this paper.

OBJECTIVE

An intent of this experimental investigation was to further understand relationships among loading characteristics (e.g. direction of applied force, dynamic vs. static, torsional vs. bending) as they affect the resultant fractures of

Figure 1 - Fracture Patterns
(Legend Notation in Parentheses)

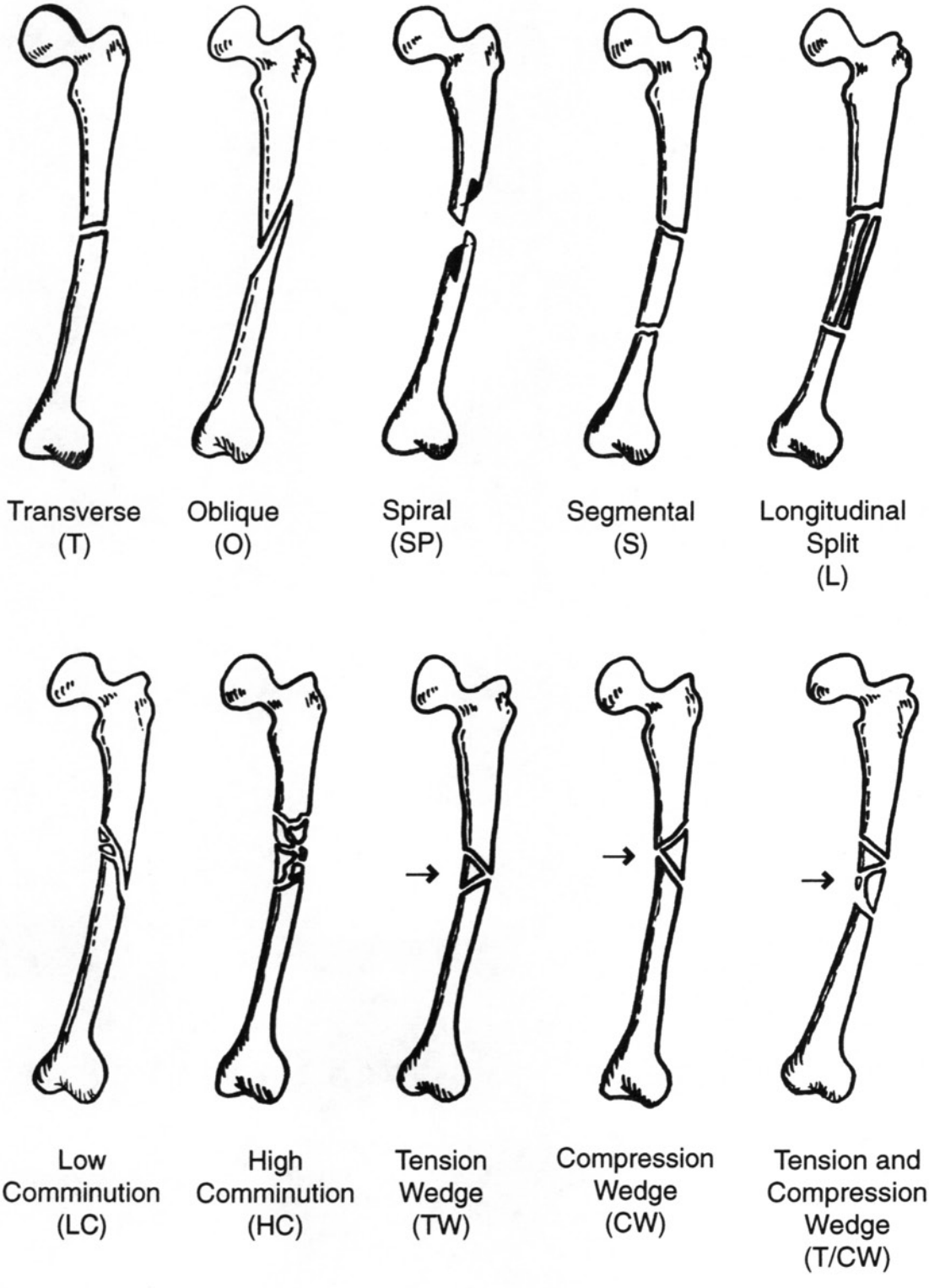

human long bones. This understanding should be useful as an aid for evaluating the effectiveness of any protective or mitigative devices or strategies. It should also be helpful in identification of all of the associated resultant injuries from a fracture. Perhaps this information could be a useful tool for accident reconstruction purposes and furthering progress with respect to emergency management for the affected individual.

EXPERIMENTAL METHOD

A total of 558 bone fracture tests are being reported on in this paper as tabulated in the appendix (Table 1). Most of the results and discussion focus on a narrowed field of these tests consisting of 253 tibias and 136 femurs. As detailed in Table 1, the specimens were obtained from a geriatric population (on the average) consisting of both males and females. All bare bones were tested in a pin-pin setup and the intact leg tests were mostly pin-inertial (foot hanging freely) or pin-friction (shoed foot on concrete block). The pin-pin setup supported the bare bones at their ends (epiphyseal aspects) and were impacted at midshaft.

Two general setups were used for the experiments. Figure 2 shows a test setup that consists of a pneumatic-based accelerator which propels a wheeled cart toward the mounted specimen. The accelerator consists of a piston assembly inside of a pneumatic chamber that is pressurized in order to achieve target velocities. For most tests the pressure was 0.34 MPa (50 psi) yielding a cart velocity of approximately 7.5 m/s. A ram connected to the piston pushed an aluminum and steel impact cart (50 kgs) throughout its stroke of approximately 1.5 meters. Then the cart separated from the ram and traveled along a railway for less than a meter before striking the specimen. In that stretch, it was timed by a photovoltaic cell/timer apparatus allowing for calculation of the velocity before impact.

Heading the cart is an instrumented 10-cm steel impactor pipe with an outside diameter of 4.13 cm. It is mounted to the front of the cart via slide pins. When contacting a specimen, the pipe was freely able to impinge on a piezoelectric quartz force transducer (PCB Piezotronics model 208A03), thereby producing a measured force equal to that which is delivered to the specimen. The transducer signal was recorded on a Hewlett Packard 3562A signal analyzer allowing storage of a force vs. time plot for each impact. However, for the purposes of this paper, discussion will focus on the resultant fracture data.

The second setup consists simply of a swinging pipe approach as shown in Figure 3. This "swinging pipe" is the same instrumented pipe that is mounted to the cart in the other setup.

After impact each specimen was examined (intact legs were also x-rayed and dissected) in order to categorize the fracture pattern. Ten patterns were observed as shown in Figures 1 and 4. The results have been grouped into logical categories as illustrated by the fifteen data charts in Figures 5 and 6. These correspond, respectively, with the first fifteen rows of Table 1. Note that all the fracture data from the swinging pipe tests (Figure 3) could be classified

into four categories (Figure 6). Considering that all of these tests were of bare bones, the data may be indicating a lower incidence of comminution as compared with the intact specimens.

Figure 2a - Wheeled Cart Setup (Showing Simply-Supported Bare Bone)

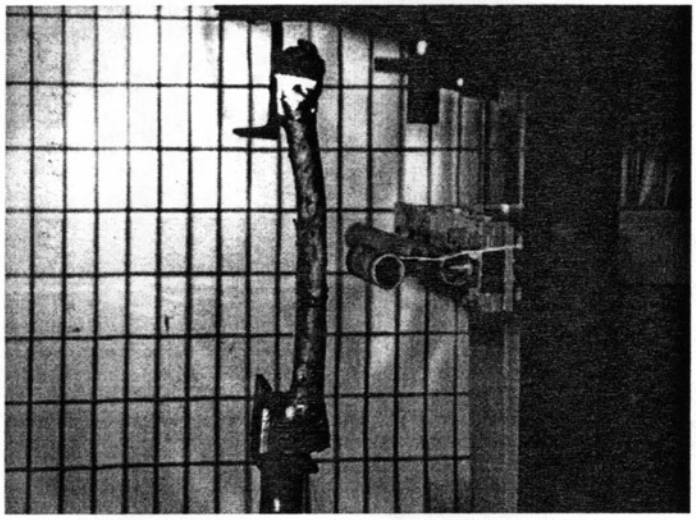

Figure 2b - Wheeled Cart Setup (Showing Impact of Intact Leg)

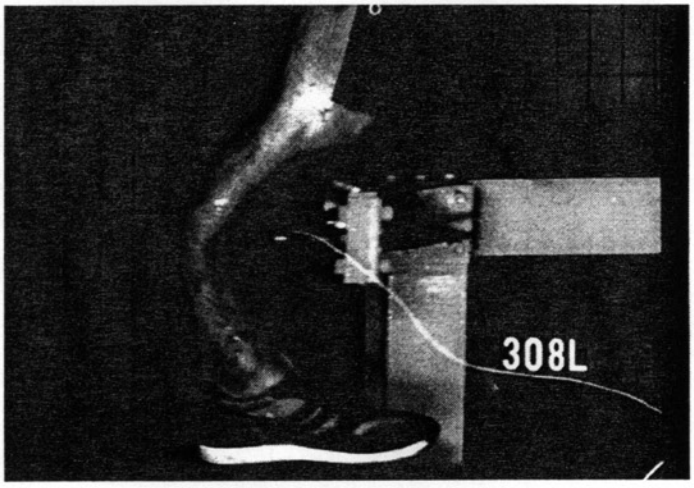

Figure 3 - Sketch Showing "Swinging Pipe" Approach

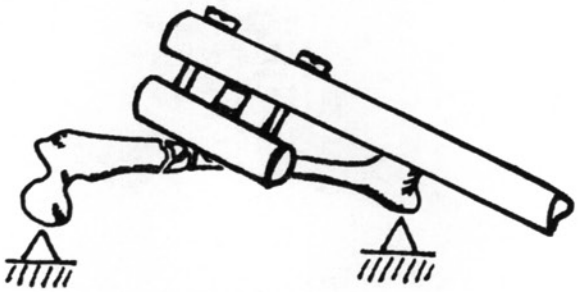

Figure 4 - Photographs of Actual Test Specimens Showing Fracture Patterns

Transverse (T)

Oblique (O)

Spiral (SP)

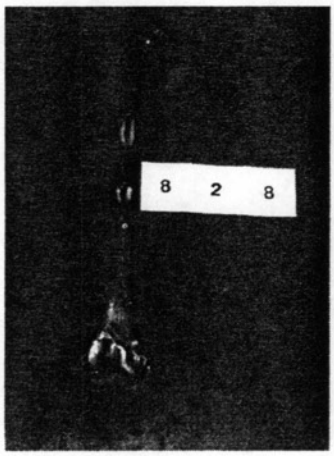

Segmental (S)

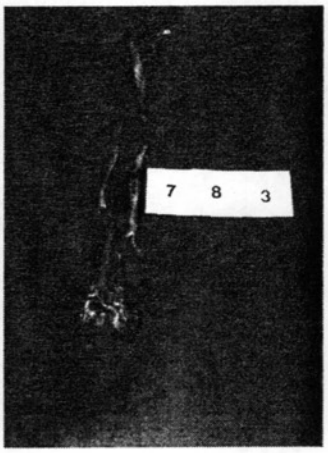

Longitudinal Split (L)

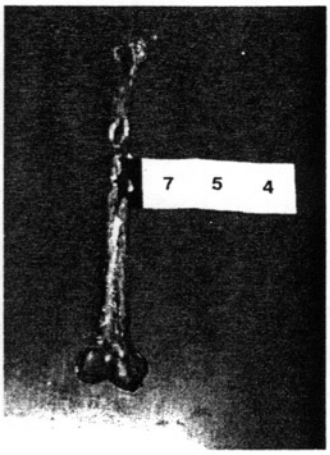

Low Comminution (LC)

High Comminution (HC)

Tension Wedge (TW)

Tension/Compression Wedge (T/CW)

Figure 5 - Fracture Patterns From Impacts Using Apparatus in Figure 2

A-P Impacted Tibia (n=95)

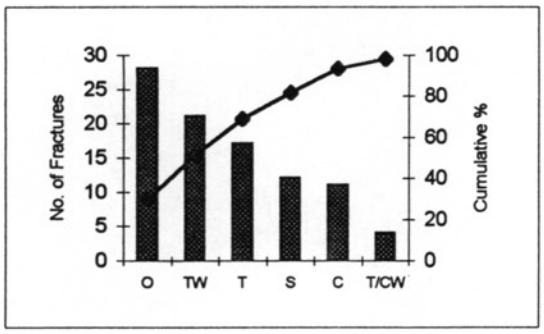

A-P Impacted Tibia Low Velocity (n=23)

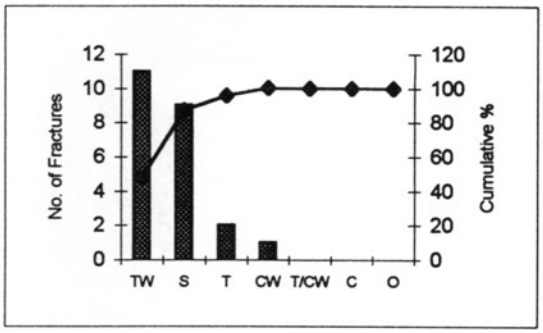

L-M Impacted Tibia (n=33)

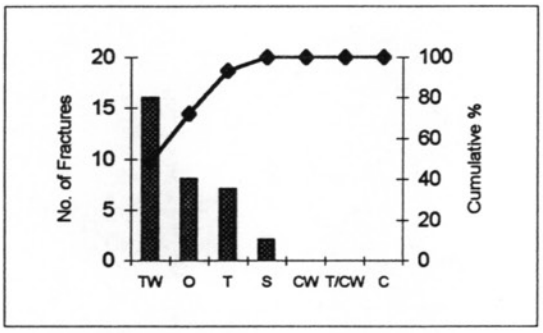

A-P Impacted Intact Leg/Tibia (n=70)

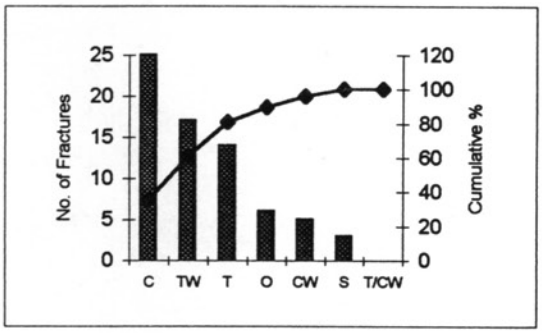

AL-PM Impacted Intact Leg/Tibia (n=9)

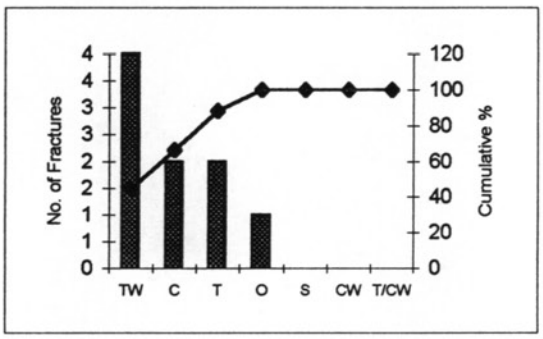

A-P Impacted Femur (n=50)

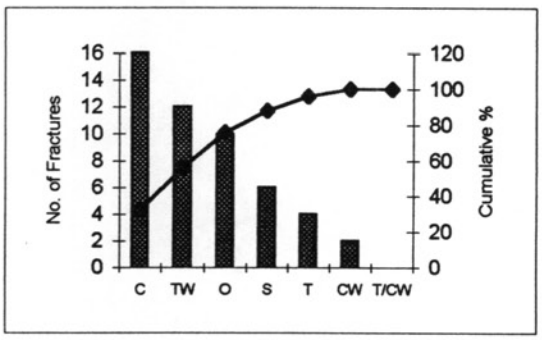

L-M Impacted Femur (n=21)

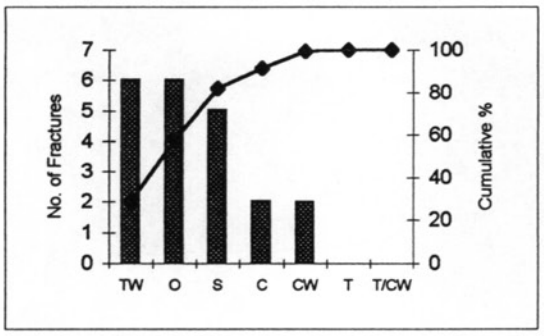

Legend

T	Transverse
O	Oblique
SP	Spiral
S	Segmental
L	Longitudinal Split
C	Comminution
TW	Tension Wedge
CW	Compression Wedge
T/CW	Tension and Compression Wedge

Figure 6 - Fracture Patterns From Impacts Using Apparatus in Figure 3

A-P Impacted Femur (n=32)

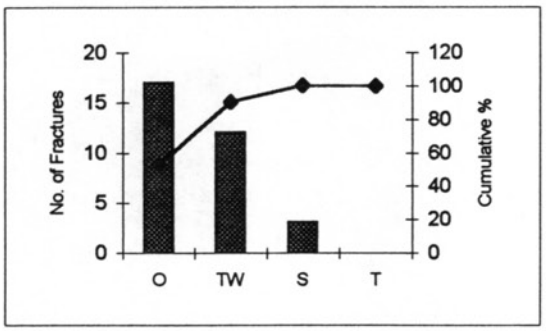

P-A Impacted Femur (n=14)

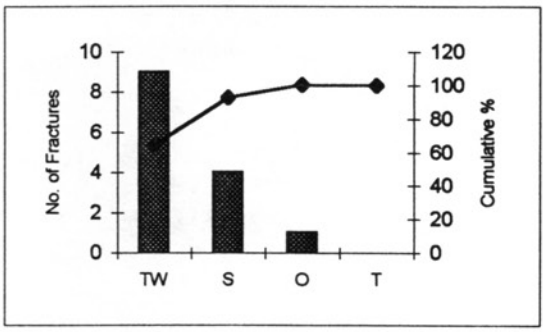

L-M Impacted Femur (n=10)

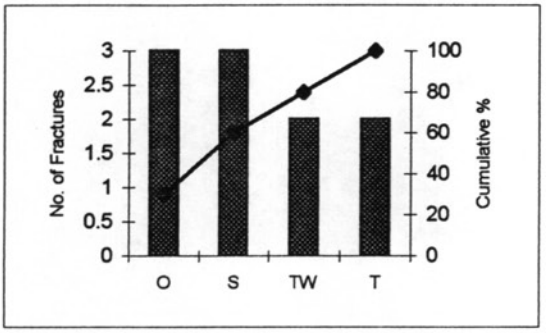

M-L Impacted Femur (n=9)

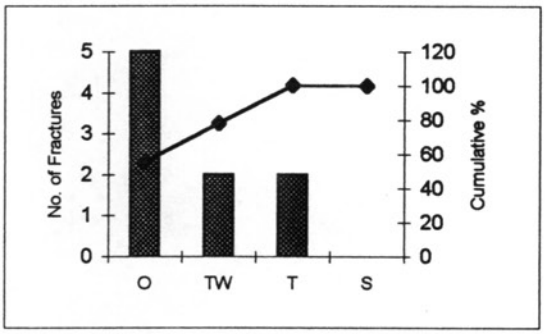

A-P Impacted Tibia (n=11)

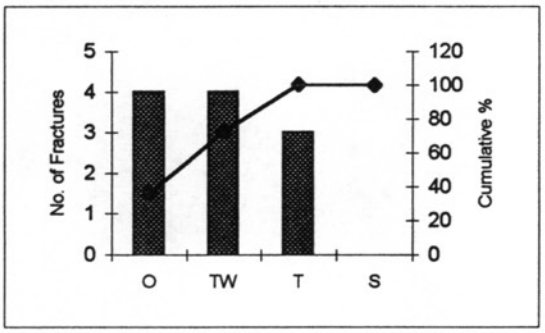

P-A Impacted Tibia (n=4)

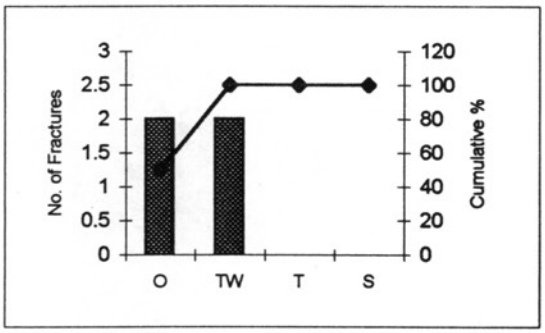

L-M Impacted Tibia (n=4)

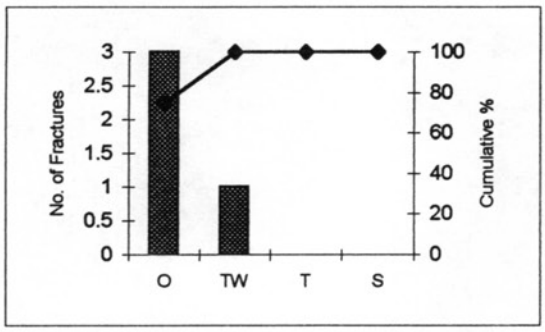

M-L Impacted Tibia (n=4)

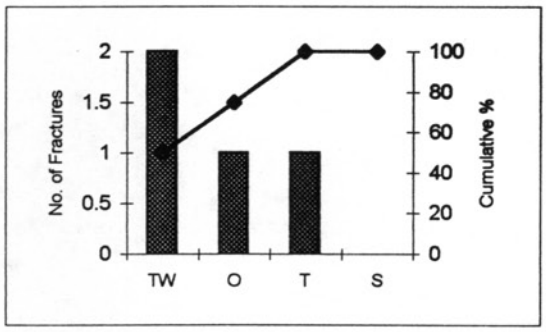

RESULTS

All of the observed patterns were produced by transverse loading of the shafts of the long bones, except for the spiral fracture which resulted only from pure torsion or from the existence of pre-torsional loading. The photographs in Figure 4 are of actual test specimens and illustrate the different patterns in the same respective order as Figure 1. A compression wedge type fracture is not included in the photographs, because it has the same appearance as a tension wedge (just rotated 180°). Figures 5 and 6 show the frequencies of occurrence of these patterns resulting from various experimental impacts. These data and other data are tabulated at the end of this paper as an appendix. Each chart in Figures 5 and 6 represents a different combination of the test parameters that include loading direction, specimen choice (tibia, femur, or intact leg), impact velocity, and test method. As noted in the figures, the direction of impact was anterior-to-posterior (A-P), posterior-to-anterior (P-A), lateral-to-medial (L-M), medial-to-lateral (M-L), or at a 45° offset angle laterally from the anterior side to the posterior/medial side (AL-PM). All impacts in Figure 5 were at a speed of approximately 7.5 m/s except for the indicated low velocity data which were at approximately 1.2 m/s. Figure 6 contains data from the swinging pipe test series in which 88 bones were fractured all at a velocity estimated to be about 5.0 m/s. This speed was approximated by digitizing twelve of the test films.

OBSERVATIONS AND CONCLUSIONS

(1) It appears reasonable to combine the data from varying loading directions (A-P, P-A, L-M, AND M-L). In other words, the resultant fracture types seem to be extremely similar regardless of the direction of the impact.

(2) Intact leg impacts promote more comminution type fractures than bare bone impacts. It is believed that the impactor continues to impart forces and energy on the intact leg bones because of the containment provided by the surrounding soft tissue. Also, the inertial constraints of the foot mass and upper leg/body components cause a wrap-around effect that results in increased comminution as the specimen stretches around the impactor.

(3) Embalmed intact leg fractures exhibit greater comminution than unembalmed. The embalment process causes significant increase in stiffness of the soft tissue containment.

(4) It is reasonable to assume that transverse, oblique, segmental, and tension wedge fractures are all just different manifestations of tensile failure. Even high comminution fractures probably originate as tensile fractures but get further fragmented due to other influences.

(5) Compressive wedge type failures are extremely rare in long bones. This is expected as human bone is approximately 1.5 times stronger in compression than it is in tension.

(6) Although the femur is stronger and has a different cross-sectional geometric shape, its fracture patterns as a result of transverse loading are generally the same as those for the tibia.

(7) The most common fracture pattern is the tension wedge and is followed closely by the oblique fracture.

(8) Transverse and oblique fractures generally have jagged edges.

(9) Spiral fractures have the "smoothest" break edge, perhaps indicating that it follows some pre-existing engineering structural line. Wedge fracture lines tend to follow curved paths similar to the spiral fracture path.

(10) Tensile wedge fractures clearly originate at a location directly opposite of the point of impact and the wedge segment radiates back through the bone initially forming a 90° vertex angle (propagates 45° from the horizontal both superiorly and inferiorly) indicating possible transition along the lines of principal stress (transition from purely tensile to shear). Refer to the illustration of the tension wedge in Figure 1 in which the arrow indicates the direction of impact. A previous report by Levine (1986) stated the opposite of what this illustration shows. He stated that the butterfly occurs on the side in which the bone is in tension implying that the "base" of the "triangle wedge" occurs on the opposite side of the impact. This is not correct for almost all cases as indicated in Table 1. Levine's work describes a compression wedge, which is an extremely uncommon pattern for long bones.

(11) The only bare bones with high comminution were those that were extremely osteoporotic or loaded axially at high speeds (e.g. a knee impact).

(12) Because of the high incidence of tension wedges, this fracture pattern can be used as an indicator of the direction of impact.

(13) Many oblique fractures also have tensile wedge patterns that are not detected by x-ray. Note the appearance of these lines in a specially treated bone in Figure 7.

(14) The fracture patterns of low speed impacts (1.2 m/s) are very similar to those of high speed (7.5 m/s) with the exception that high comminution is not observed in the low speed fractures. This is somewhat of a unique observation because it has been commonly thought that the butterfly wedge results only from high speed impacts.

(15) Spiral fractures only appear when the bones are subjected to torsional loads. Furthermore, if long bones are loaded in pure torsion then spiral fractures will result 100% of the time. Previous researchers, Kramer et al (1973), reported that the absence of spiral fractures from transversely loading long bones of geriatric humans was due to the fact that older people have more brittle bones. This is not the case. A transverse load is simply not a causal mechanism of a spiral fracture.

(16) Approximately two out of three spiral fractures of the femur were located at the proximal third.

(17) A torsional loading direction is herein defined as being "clockwise" if the top is held and the bottom is twisted in the clockwise direction (looking up). Contrary to popular belief, a clockwise torsional load will result in the spiral portion of the fracture being oriented like a right-hand screw (see Figure 8). For example, the spiral fracture illustrated in Figure 1 would have been loaded torsionally in the counterclockwise direction. This interesting observed fracture behavior is indicative that the bone is failing in tension rather than shear when loaded in torsion.

(18) Segmental fractures are much more prevalent in femurs than tibias.

(19) Transverse loading to the tibia/fibula most often results in a segmental fracture of the fibula.

(20) Surfaces of eight bones were videographically scanned and stored in the computer prior to their impact tests. Post-test examination of the fractures and stored computer images provided no evidence of the presence of surface stress risers that could have caused fracture or crack propagation.

(21) Fractures resulting from 7.5 m/s impacts can be quite serious, that is causing significant injury. This conjecture is also supported by research pertaining to pedestrian injury and vehicle design by Pritz and Hassler (1975).

(22) Pritz and Hassler also reported no noticeable differences in injury severity associated with cylindrical impactor radius changes from 1-inch to 4-inches. This is consistent with the findings in this study.

(23) Comminuted fractures can occur without entrapment (crushing injury). For 7.5 m/s impacts of intact legs, the inertial restraint of the tibia from the upper thigh and foot is sufficient enough to result in comminuted fractures without any additional support. For low speed tests (static and 1.2 m/s), simply-supported legs have resultant bone fractures comparable to inertially supported legs at high speeds.

(24) Age changes in bone can exist, although these changes do not seem to significantly affect fracture patterns (except when compared to babies or small infants). Such changes can include mineral mass, volume, density, and mechanical properties. During dynamic loading situations when ultimate strength is exceeded, bone basically fails as a brittle material (young or old). So, the fractured patterns do not vary too much, unless severe osteoporitic changes have occurred. Such osteoporosis can increase the incidence of high comminution (shatter).

(25) For impact loading of the long bone shaft, arthritic changes did not seem to affect the resultant fracture pattern of the entire bone. In other words, a fair supposition would be that arthritis only affects failure patterns when they involve joints.

Figure 7 - Fractured Bone After Special Treatment Showing Tensile Wedge Stress Fractures

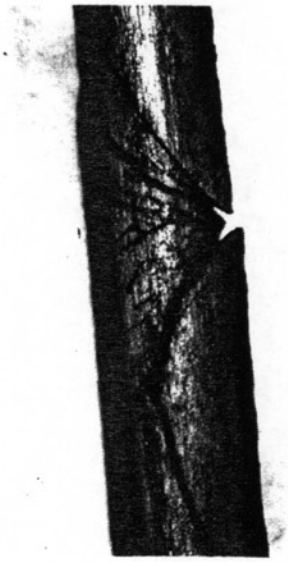

Figure 8 - Relationship Between Torsional Loading Direction and Resultant Spiral Fracture Direction

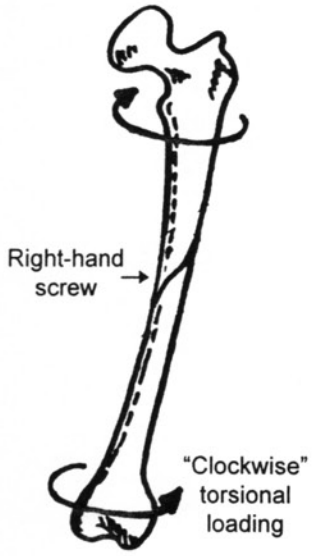

BIBLIOGRAPHY

1. Cowin, S.C. **Bone Mechanics.** CRC Press, Inc. New York, New York: 1989.
2. Dellinger, E.P., et al. "Risk of Infection After Open Fracture of the Arm or Leg." **Arch Surg.** Volume 123: Nov 1988.
3. Evans, F.G. **Stress and Strain in Bones.** Charles C. Thomas Publisher. Springfield, Illinois: 1957.
4. Evans, F. G. and Lebow, M. "The Strength of Human Compact Bone as Revealed by Engineering Technics." **Am. J. Surg.** Volume 83, pp. 326-331: 1952.
5. Evans, F. G. and H.R. Lissner. "Stresscoat Deformation Studies of the Femur Under Vertical Static Loading." **Anat. Rec.** Volume 101, pp. 225-241: 1948.
6. Frost, H.M. **The Laws of Bone Structure.** Charles C. Thomas Publisher. Springfield, Illinois: 1964.
7. Gustilo, R.B. **The Fracture Classification Manual.** Mosby Year Book: 1991.
8. Heckman, J.D. "Fractures." **Clinical Symposia.** Volume 43, Number 3. Ciba-Geigy: 1991.
9. Kramer, M., K. Burow, and A. Heger. "Fracture Mechanism of Lower Legs Under Impact Load." SAE technical paper #730966. Society of Automotive Engineers, Inc.: 1973.
10. Kress, T.A. **Mechanical Behavior of the Human Lower Limb to Impact Loading: Facility Development and Initial Results.** Masters Thesis. University of Tennessee. Knoxville, Tennessee: 1989.
11. Kress, T.A., et al. "Automobile/Motorcycle Impact Research Using Human Legs and Tibias." **Rider-Passenger Protection in Motorcycle Derivative Vehicles in Traffic Accidents.** SAE International Congress and Exposition. Detroit, Michigan: 1990.
12. Kress, T.A., et. al. "Determination of Lower Limb Failure Modes and Tissue Damage by Impact Loading." **Proceedings of the 6th International Congress on Experimental Mechanics.** Portland, Oregon: 1987.
13. Kress, T.A., D.J. Porta, et al. "Human Femur Response to Impact Loading." **Proceedings of the International Research Council on Biokinetics of Impacts.** Netherlands. pp. 93-104: 1993.

14. Levine, R.S. "An Introduction to Lower Limb Injuries." **Biomechanics and Medical Aspects of Lower Limb Injuries.** SAE technical paper #861922. Society of Automotive Engineers, Inc. pp. 23-29: 1986.

15. Messerer, O. **Uber Elasticitat und Festigkeit der menschlichen Knochen.** Stuttgart, Cotta. pp. 1-100: 1880.

16. Pike, J.A. **Automotive Safety: Anatomy, Injury, Testing, & Regulation.** Society of Automotive Engineers, Inc.: 1990.

17. Porta, D.J., T.A. Kress, P.M. Fuller, and J.N. Snider. "Impact Studies of Embalmed Human Cadaver Thighs and Femurs." **Proceedings of the 14th International Technical Conference on the Enhanced Safety of Vehicles (ESV).** Munich, Germany. Volume 1, pp.. 299-304: 1994.

18. Porta, D.J., T.A. Kress, et al. "Dynamic Impacting of Embalmed Versus Unembalmed Human Cadaver Legs." **Proceedings of the 22th Annual International Workshop on Human Subjects for Biomechanical Research.** Fort Lauderdale, Florida. pp. 135-144: 1994.

19. Porta, D.J., T.A. Kress, et al. "Biomechanics of Impacting Human Cadaver Thighs." **The Anatomical Record.** San Diego, California. Supplement Number 1. p.96: 1993.

20. Pritz, H.B., et al. "Experimental Study of Pedestrian Injury Minimization Through Vehicle Design." SAE technical paper #750166. Society of Automotive Engineers, Inc.: 1975.

21. Rauber, A.A. "Elasticitat und Festigkeit der Knochen." Leipzip, Wilhelm Engelmann. iv, pp. 1-75: 1876.

22. Roth, A.I., et al. "Infectious Morbidity in Extremity Fractures." **Journal of Trauma.** Volume 26, Number 8: 1986.

23. Snider J.N., J.F. Wasserman and T.A. Kress. "The Response of the Human Lower Leg to Impact Loading." **Proceedings of the International Research Council on the Biokinetics of Impacts**, Bergisch-Gladbach (FRG): 1988.

ACKNOWLEDGMENTS

This work was mainly sponsored by the Japan Automobile Manufacturers Association, and in part by The University of Tennessee and The University of Louisville School of Medicine.

APPENDIX

The following table summarizes the data collected with regard to the dynamic response characteristics of human long bones. As mentioned earlier, the seven charts contained in Figure 5 correspond to the first seven rows of this table, and the next eight rows correspond to the data in the charts for Figure 6.

Table 1 - Summary Data of the Dynamic Response Characteristics of Human Long Bones

Specimens were embalmed and impacted at midshaft while simply supported, unless noted otherwise.

Impact Plane & Specimen	Impactor	Male Mean Force kN (Std. Dev.)	Female Mean Force kN (Std. Dev.)	Average Velocity m/s (Std. Dev.)	n	Fracture Classifications			Cadaver Information (% Sex - Avg Age)
A-P Tibia	Pipe	4.85 (2.08)	3.60 (1.72)	7.5 (0.35)	95	29.5% Oblique 12.6% Segmental 2.1% Tension/Compression Wedge	22.1% Tension Wedge 11.6% Comminuted	20.0% Transverse 2.1% Compression Wedge	52.4% M - 69.6 47.6% F - 74.6
A-P Tibia (Low Vel)	Pipe	2.21 (0.91)	1.86 (0.85)	1.5 (0.59)	23	47.8% Tension Wedge 4.4% Compression Wedge	39.1% Segmental	8.7% Transverse	52.3% M - 77.0 47.7% F - 82.3
L-M Tibia	Pipe	4.07 (1.22)	2.91 (1.31)	7.7 (0.28))	33	48.5% Tension Wedge 6.1% Segmental	24.2% Oblique	21.2% Transverse	42.4% M - 74.3 57.6% F - 78.9
A-P Intact Leg/Tibia	Pipe	6.96 (2.62)	5.08 (2.51)	7.3 (1.41)	70	35.7% Comminuted 8.6% Oblique	24.3% Tension Wedge 7.1% Compression Wedge	20.0% Transverse 4.3% Segmental	50.0% M - 76.7 50.0% F - 75.8
AL/PM Intact Leg/Tibia	Pipe	8.45 (0.57)	4.11 (1.16)	7.3 (0.22)	9	44.4% Tension Wedge 11.2% Oblique	22.2% Comminuted	22.2% Transverse	37.5% M - 82.7 62.5% F - 72.0
A-P Femur	Pipe	5.70 (2.68)	4.58 (1.45)	7.4 (0.46)	50	32.0% Comminuted 12.0% Segmental	24.0% Tension Wedge 8.0% Transverse	20.0% Oblique 4.0% Compression Wedge	52.3% M - 69.2 47.7% F - 72.6
L-M Femur	Pipe	5.48 (1.17)	3.05 (2.12)	7.5 (0.35)	21	28.6% Tension Wedge 9.5% Comminuted	28.6% Oblique 9.5% Compression Wedge	23.8% Segmental	28.6% M - 71.0 71.4% F - 76.8
A-P Femur	Pipe	2.67 (1.67)	2.10 (1.38)	5.0[1]	32	53.1% Oblique	37.5% Tension Wedge	9.4% Segmental	32.3% M - 75.4 67.7% F - 75.8
P-A Femur	Pipe	2.48 (0.69)	1.45 (0.65)	5.0[1]	14	64.3% Tension Wedge	28.6% Segmental	7.1% Oblique	42.9% M - 83.5 57.1% F - 79.5
L-M Femur	Pipe	4.75 (4.07)	3.14 (na)	5.0[1]	10	30.0% Oblique 20.0% Tension Wedge	30.0% Segmental	20.0% Transverse	88.9% M - 69.3 11.1% F - 73.0
M-L Femur	Pipe	2.29 (1.25)	1.61 (1.08)	5.0[1]	9	44.4% Oblique	33.3% Transverse	22.3% Tension Wedge	75.0% M - 76.3 25.0% F - 81.0
A-P Tibia	Pipe	2.96 (1.79)	1.35 (0.32)	5.0[1]	11	36.4% Tension Wedge	36.4% Oblique	27.2% Transverse	54.5% M - 75.0 45.5% F - 70.6
P-A Tibia	Pipe	na	1.12 (0.78)	5.0[1]	4	50.0% Tension Wedge	50.0% Oblique		100.0%F - 84.0
L-M Tibia	Pipe	1.02 (0.35)	na	5.0[1]	4	75.0% Oblique	25.0% Tension Wedge		100.0% M - 68.3

Impact Plane & Specimen	Impactor	Male Mean Force kN (Std. Dev)	Female Mean Force kN (Std. Dev.)	Average Velocity m/s (Std. Dev.)	n	Fracture Classifications	Cadaver Information (% Sex - Avg Age)
M-L Tibia	Pipe	1.89 (na)	1.72 (0.66)	5.0[1]	4	50.0% Tension Wedge 25.0% Oblique 25.0% Transverse	25.0% M - 85.0 75.0% F - 82.3
Torsion of Humeri	na	56.05 N-m (19.20)	11.96 N-m (3.75)	na	6	100% Spiral Fractures	66.7% M - 74.5 33.3% F - 77.0
Torsion of Tibia/fibulas	na	91.96 N-m (51.09)	na	na	4	100% Spiral Fractures	100% M - 76.3
Torsion of Femurs	na	106.72 N-m (23.78)	96.68 N-m (39.36)	na	33	100% Spiral Fractures	63.0% M - 72.8 37.0% F - 78.0
A-P Fibula	Pipe	2.15 (1.27)	0.93 (0.68)	7.4 (0.63)	25	Most were Segmental or Comminuted	80.0% M - 74.5 20.0% F - 60.8
P-A Humerus	Pipe	4.88[3] (0.58)	na[3]	6.9 (0.21)	2	50.0% Tension Wedge 50.0% Oblique	Unknown
A-P Tibia	Plate	4.20 (2.11)	4.21 (1.67)	7.5 (0.12)	25	32.0% Tension Wedge 28.0% Segmental 20.0% Comminuted 8.0% Oblique 8.0% Compression Wedge 4.0% Transverse	56.5% M - 67.0 43.5% F - 68.6
L-M Fibula	Pipe	1.15 (0.52)	0.57 (0.28)	7.8 (0.29)	21	Mostly Wedge, Oblique and Segmental	52.4% M - 72.5 47.6% F - 78.4
L-M Femur Pre-Torque[2]	Pipe	3.03[3] (1.83)	na[3]	6.9 (0.25)	10	40.0% Spiral 30.0% Segmental 20.0% Comminuted 10.0% Oblique	Unknown
Axial Femur	Plate	8.38 (1.94)	6.20 (1.83)	6.8 (0.94)	10	Fractures of the Neck in 80%, Shaft in 40% and Knee in 20% (Percentages are >100 due to multiple fractures per specimen)	50.0% M - 63.8 50.0% F - 67.0
Axial Femur	MTS	5.42 (3.02)	4.99 (1.22)	Static	9	88.9% Neck Fracture 11.1% Subtrochanteric Fracture	66.7% M - 66.5 33.3% F - 71.7
Axial Intact Knee	Plate	9.47 (1.78)	8.46 (na)	7.5 (0)	5	60.0% Fracture of Patella only 40.0% Comminuted Fractures of Patella, Tibia and Femur	80.0% M - 88.5 20.0% F - 73.0
Axial Intact Knee	Pipe	9.87 (1.42)	8.37 (3.37)	7.5 (0)	7	85.7% Comminuted Fractures of Patella, Tibia and Femur 14.3% Fracture of Patella only	28.6% M - 89.0 71.4% F - 75.4
A-P Intact Thigh	Pipe	8.23 (na)	5.00 (0.93)	7.5 (0)	6	50.0% Wedge 50.0% Oblique 16.7% Transverse 16.7% Neck Fracture (Percentages are >100 due to multiple fractures per specimen)	50.0% M - 81.3 50.0% F - 87.0
L-M Intact Thigh	Pipe	6.98 (2.20)	5.37 (1.20)	7.5 (0)	6	100% Comminuted 16.7% Neck Fracture (Percentages are >100 due to multiple fractures per specimen)	50.0% M - 81.3 50.0% F - 87.0

[1] A velocity of 5.0 m/s is an estimate based on video analysis of pipe swing speeds.
[2] These femurs were subjected to a pre-torque of 10.06 or 20.14 N-m during impact..
[3] Sex was unknown for this group, data was placed in the column for Males out of convenience.